IEEE Access
Multidisciplinary | Rapid Review | Open Access Journal

Received August 6, 2019, accepted September 11, 2019, date of publication October 7, 2019, date of current version October 21, 2019.

Digital Object Identifier 10.1109/ACCESS.2019.2945983

Surface-Property Recognition With Force Sensors for Stable Walking of Humanoid Robot

SANDIP BHATTACHARYA, AIWEN LUO, (Member, IEEE), TAPAS KUMAR MAITI, (Member, IEEE), SUNANDAN DUTTA, YOSHIHIRO OCHI, MITIKO MIURA-MATTAUSCH, (Fellow, IEEE), AND HANS JÜRGEN MATTAUSCH, (Senior Member, IEEE)

HiSIM Research Center, Hiroshima University, Hiroshima 739-8530, Japan

Corresponding author: Aiwen Luo (luoaiwen@hiroshima-u.ac.jp)

This work was supported by the Hiroshima University TAOYAKA Program for creating a flexible, enduring, peaceful society, funded by the Program for Leading Graduated Schools, Ministry of Education, Culture, Sports, Science and Technology.

ABSTRACT In this paper, we propose a surface-identification system for stable humanoid-robot walking on various types of surfaces using force sensors mounted under the robot feet. For experimental identification analysis of the surface condition, we measured the sensor-output data using five different types of test surfaces. To achieve fast dynamic recognition capability of changing surface conditions, we applied an overlapped sliding-window method for the incoming sensor-data stream to generate dynamically four distinguishable well-known features from the raw sensor data. The multi-class k-nearest-neighbor (MC-kNN) classifier rather than a binary classifier is used for online classification of the measured robot-walking pattern and classification-accuracy evaluation. Further, we combine the four studied feature descriptors into a fused multi-feature descriptor rather than invoking each feature descriptor independently, increasing the classification performance. Our analysis results verify that 90.4% maximum overall accuracy with 91.49% average precision can be achieved, demonstrating the realization of a better cost-performance trade-off than in other previous research works. The obtained results are useful for balancing the robot body through optimized controlling of the robot motors according to the recognized different surfaces during robot motion.

INDEX TERMS Humanoid robot, force sensor, sliding-window method, multi-class classification, surface identification, walking-pattern recognition.

I. INTRODUCTION

A. BACKGROUND

Surface identification is one of the most important elemental tasks of humanoid robots operating in a harsh environment for enabling the maintenance of their dynamic balance. With the identification of the surface type, a small and portable humanoid robot becomes a good option, which can better navigate through such environments as compared with other robot types (e.g. wheel robots). While most of the robotic researchers used cameras, range sensors, or ground-penetrating radar, etc., for surface identification purposes, force sensing can provide a cost-effective and potent solution to solve this problem by accumulating information, precisely related to the mechanical properties of various types of surfaces (for example properties like hard, soft, smooth and rough). The force-sensor-collected surface-property information is usually sent to the robot controller for determining the surface-pattern-related control mode of stable robot walking.

The associate editor coordinating the review of this manuscript and approving it for publication was Xian Sun.

B. RELATED WORKS

Over the last few decades, a number of surface-identification methods have been developed to classify different types of surfaces and have been applied in application-specific robots. Inertial sensors are reported in [1] and [2] for surface tracking of wheeled robots. Here, the wheels of the robot vehicles are acting as the sensing material. However, the surface information collected by such types of assembled systems is bounded by the mechanical response itself. A tactile-probe (metallic rod) sensor for surface and terrain identification of mobile robots is reported in [3]. Here, ten different surface types are considered for generating a sensory signal to detect the surface type with high accuracy. A rigidity-based surface identification using a legged robot and ground-contact force sensors is reported in [4], where the authors have considered six different types of indoor surfaces. The random-forest

classifier is used for surface identification, achieving an accuracy of around 94%. Walas *etal.* [5] reported a terrain-classification method for a walking robot with the ability to identify twelve different types of terrain surfaces using vision, depth and tactile sensors. The SVM classifier is used to analyze the surface detection by collecting the information from each sensor, thus reaching 94.44% precision. A similar terrain classification for a legged robot is reported by Hoepflinger *etal.* [6]. The surface properties and different terrain shapes are extracted from joint-motor current and ground-contact-force sensors. The AdaBoost machine-learning classifier is used to extract the features of the surface with 94% accuracy for a single-leg test bed. The surface detection using a quadruped robot is reported in [7]. Accelerometer and paw sensors are used to detect two different types of surface (wood flooring and vinyl flooring). Here a naive Bayes classifier is used to achieve recognition accuracy of 85-91%. A vision-based surface-identification method using spectral-camera and laser-range-finder (LRF) was reported in [8] and [9]. The aforementioned work is based on multi-leg and wheel-robot investigations including tactile and vision-based sensors. Apart from the above broader work, some specific research on biped robots for surface identification with several classifier techniques has already been done. Research on dynamic and stable walking in compliant contact environment for biped robots (ANR-SHERPA-French national project) using force sensors is reported in [10].

A simulation-based control architecture is developed to stabilize robot walking by generating specific walking patterns for different surface conditions. A similar type of work was reported in [11]. High-speed pressure-sensing capability for humanoid-robot walking using force sensors and advanced scanning circuitry is reported in [12]. The authors have mainly highlighted their work on high-speed dynamically-distributed pressure-detection, measurements and center-of-pressure (CoP) trajectory calculations using a pressure-sensor grid on smooth conductive rubber surfaces (only for flat surfaces and staircases) achieving a highly stable walking condition. The terrain classification using force/torque sensors mounted on the ankles of a humanoid robot is reported in [13]. The WALK-MAN humanoid robot is used to collect experimental data from five different types of surfaces. Fast Fourier Transform (FFT) and Discrete Wavelet Transform (DWT) are used to classify the terrain pattern with high precision and recall rate of both about 95%. However, in most of these reported works, the surface patterns are assumed to be known previously. There are several research works that have been carried out based on contact-force measurements using resistive [14]–[16], capacitive [17], [18] and inductive [19], [20] sensors. Among these, inductive sensors are bulky in size and thickness, whereas capacitive sensors are very expensive and sophisticated for low contact-force measurement. Compared with inductive and capacitive sensors, a piezo-resistive sensor is useful for robust and low-cost applications.

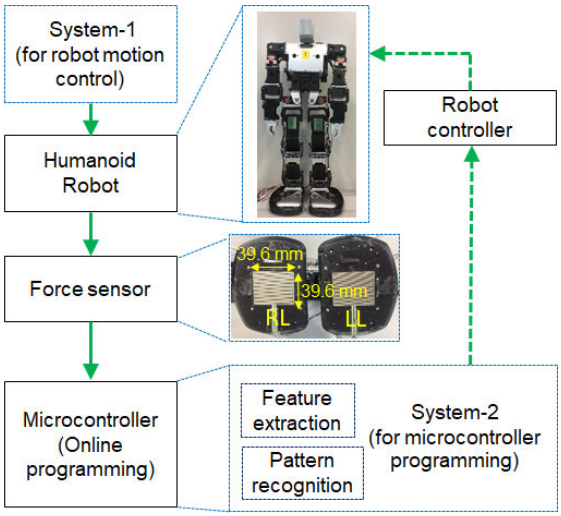

FIGURE 1. Overall system design for detecting different types of surface patterns (soft, hard, smooth and rough), using the humanoid robot Kondo KHR-3HV and force sensors.

C. CONTRIBUTIONS

Motivated by the previous works, we have implemented a low-cost surface-pattern detection and recognition system, using a humanoid-robot and force-sensors, which can detect the different types of walking surfaces dynamically. The structure of the on-line detection system, as is illustrated in Fig. 1, consists of the Kondo KHR-3HV humanoid robot [22], two membrane force sensors [23] attached under both robot feet, a programmable microcontroller implemented by an Arduino-UNO board, a robot controller embedded in the robot and the corresponding overall control system installed on a PC.

For recognizing the walking patterns corresponding to different types of flat walking surfaces in real time, we extracted feature vectors from the raw data of the force sensors and employed the Euclidean distance to search the closest neighbor to the given reference patterns for classification.

We employed four kinds of time-domain descriptors for extracting the feature vectors, which describe the critical information of our biped robot's dynamic walking patterns in an optimized way. To the best of our knowledge, we propose a novel sliding-window algorithm for dynamic feature extraction from serially streamed force-sensor data, enabling online surface identification, with very small consumption of memory resources (32 kB flash on-board memory). A 1/2 -stride sliding window is employed in this work, which reduces the processing time for real-time applications relative to a complete-stride window size.

Four different feature descriptors were evaluated independently using the k-nearest neighbor (kNN) classifier for multi-class problems, to enable consideration of a variety of walking surfaces in real-world environments, rather than using multiple binary classifications (i.e., a one-versus-one strategy) with all combinational pairs of two walking surfaces. In other words, the multi-class problem is treated in a one-versus-all (OVA) approach for performance evaluation of

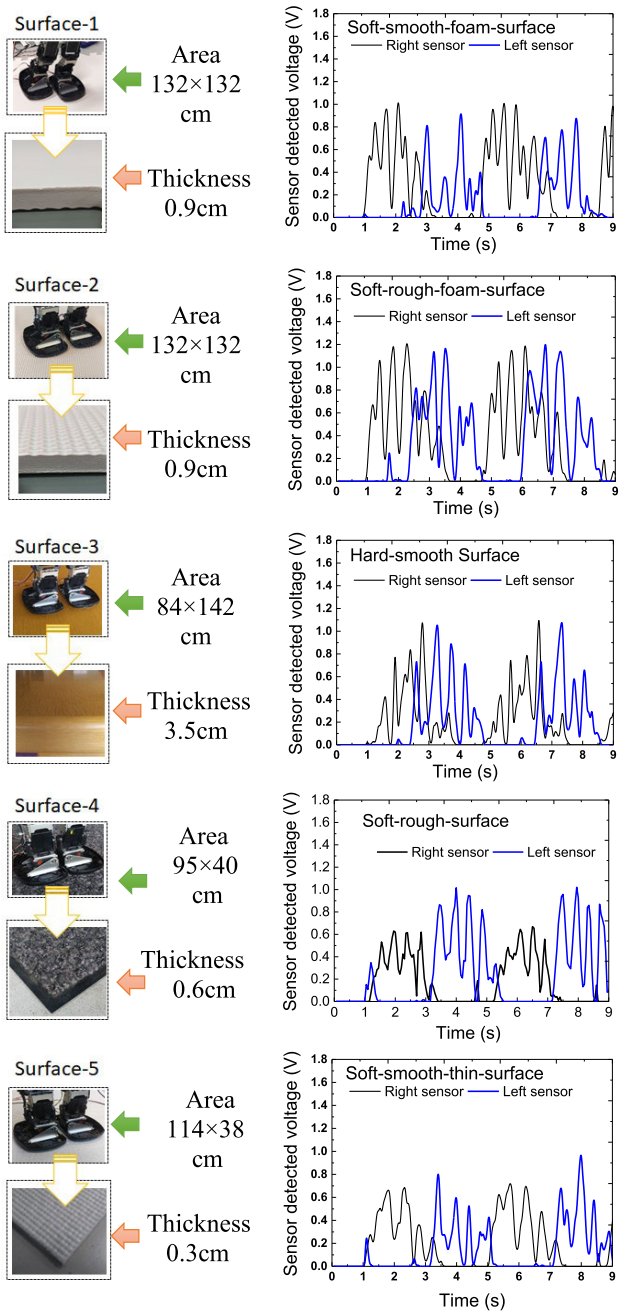

FIGURE 2. Sensor detected voltage during robot walking. (a) Surface-1 represents a soft-smooth foam surface, (b) Surface-2 represents a soft-rough foam surface, (c) Surface-3 represents a hard-smooth surface (wooden surface), (d) Surface-4 represents a soft-rough surface (carpet), (e) Surface-5 represents a soft-smooth thin surface (thin carpet).

the proposed classification model with more than two classes. Further, we combined the four features into a multi-feature descriptor with the multi-class kNN strategy to increase the classification performance.

Various experimental situations on five kinds of different walking surfaces were measured for the biped robot, and the system performances was compared with state-of-the-art previous achievements in terms of accuracy and precision. The maximum multi-class accuracy up to 90.4% is achieved by employing an integrated multi-feature descriptor when the biped robot is walking on a smooth, flat foam surface (i.e., surface-1 in Fig.2) using 125 testing samples. An average precision of 91.49% is achieved for walking-pattern recognition with the integrated multi-feature descriptor on five given surfaces. Confusion matrices for multi-class recognition are also employed to visualize more detailed analysis results than the mere classification accuracy. An important result is that this work realizes a better cost-performance trade-off than other previous research works.

D. STRUCTURE

The paper is organized as follows. Section II describes the overall structure of our proposed system for dynamic walking-pattern recognition. Section III introduces the experimental setup. Section IV describes the feature-extraction algorithm. Section V describes the online walking-pattern recognition method, followed by the experimental-result presentation, the model analysis and the comparison with other work in Section VI. Conclusions are drawn in Section VII.

II. DEVELOPED SYSTEM

The proposed system is developed for a stable walk of humanoid robots on various types of flat surfaces based on the estimation of tactile properties from force sensors, helping the biped robots to enhance their understanding of the human living environment.

Figure 1 shows the overall architecture of our developed system for surface-condition recognition based on force sensors during walking of the humanoid robot. The critical parts of our system include force sensors mounted under the two feet of the biped robot, a microcontroller applied for on-line programming of both feature extraction and pattern recognition basing on the real-time raw data inputted from the force sensors, and the robot-internal controller.

The Kondo KHR-3HV humanoid robot [22] with 1.5 kg weight, 40.11 cm height, and 17 active servo-motors, is used for our ongoing experiments. Here, System-1 (personal computer) is used to control the robot walking motion on different types of surfaces. Two membrane force sensors (piezo-resistive) [23] with 39.6×39.6 mm active area are placed under the two feet of the robot for sensory-data collection, as shown in Fig.1.

During robot walking, the force sensors are touching on the surface and generate a mechanical-strain-equivalent voltage using their piezo-resistive properties. The equivalent voltage is analog in nature and transferred to the microcontroller for conversion to a discrete digital raw-data stream, using System-2 (personal computer) via an online program. In our experiment, we employed an ATmega328P microcontroller, which is embedded in the Arduino-UNO board, for data processing.

After extracting the large sensory-data stream from the force sensor, it is transformed into a reduced set of features for the walking pattern. The main purpose of feature extraction is

to efficiently represent the characteristics of different surface types during walking by more concise information, which filters the redundant data and randomly interfering noise so that the robot can easily recognize the surface type with a lower computational cost. We employed the kNN classifier for pattern recognition, because it had to be implemented on a resource-limited microcontroller where advantage of its repetitive calculation similarity could be taken, and because of the significant classification performance. Based on the recognition results, the biped robot can send the corresponding instructions to the robot controller to make walking-mode decisions, such as changing the rotation degrees of the robot's servomotors.

In this work, our proposed system mainly focuses on real-time recognition of the characteristic walking pattern of a humanoid robot on different types of surfaces with high accuracy and fewer hardware resources.

III. EXPERIMENTAL SETUP

A. DIFFERENT TEST SURFACES

Test-surface selection is one of the critical tasks for the robot's dynamic-motion investigation. Some latest surface-related robot-walking concepts are reported in [4], [7], and [13]. Our proposed experimental setup involves five different types of surfaces where the robot can walk steadily without falling (shown on the left side of Fig.2). By changing the surface properties, such as smoothness or roughness, implies a variation in sensor-data output, as shown in Fig.2. The sensor-detected force is represented in terms of a series of discrete voltage signals. Each of the surface properties (area and thickness) is also highlighted in Fig.2.

- Surface-1: soft-smooth foam surface
- Surface-2: soft-rough foam surface
- Surface-3: hard-smooth surface (wooden surface)
- Surface-4: soft-rough surface (carpet)
- Surface-5: soft-smooth thin surface (thin carpet)

We have placed the biped robot to walk on these five different surfaces for dynamic walking-pattern recognition. Large amounts of force-sensory data are collected for classification verification of the recognition model as well.

As shown in Fig.2, the responses represented by the raw sensory data are slightly different from each other when the biped robot is walking on different surfaces. The valid force-sensory data of the two feet are alternately outputted from the force sensors when the biped-robot feet strike the five different surfaces. This work maps the measured sensory activity, corresponding to the touched surface, to a certain walking pattern of the biped robot, thus aiming to detect the slight differences among various surfaces and finally to recognize the surface-specific walking pattern of the robot in real time.

B. SENSORS

Nowadays, the tactile sensors are extensively used in robotics application for surface-pattern recognition and detection, considering robot-body vibration during dynamic motion. The performance of such kind of sensors is application-oriented. For example, a low-cost accelerometer is used to measure the body oscillation during dynamic motion with 120 Hz sampling rate for four-legged robots, as reported in [1], [3], [5], and [7]. However, advanced force sensors are very useful for surface classification and feature extraction. Most of the force sensors are attached at the edge of the robot leg to measure the foot-contact force with 10 Hz sampling rate [5], [6], and [21].

In our experimental setup, we used low-cost, ultra-thin, flexible and velocity-sensitive membrane force sensors with 39.6×39.6 mm active area, which are operated in a voltage range of $0 \sim 5$V with sufficiently short response time (<1ms), to measure inertial forces acting on the robot during walking. The sensors are mounted on the bottom of each foot of the biped robot to utilize the larger amount of active area to get accurate force-sensitive information for feature extraction and walking-pattern recognition on various surfaces, as shown in the Fig. 1. The used force sensors convert the changing contact forces from the walking surfaces to continuous voltage signals, i.e., analog signals. In the proposed system, as illustrated in Fig. 1, the microcontroller samples a number of time points for each walking step of the robot at a certain sampling rate for walking-pattern recognition in real time.

C. SAMPLE COLLECTION

Sample collection of raw-sensory data from the force sensors is the primary step for implementation and verification of our recognition model for the biped robot walking in the real environment. The large streams of serial raw-sensory data are then utilized for extracting identifiable feature vectors. During the sample collection, each walking step of the biped robot is considered as one stride and its corresponding sensory data are collected as samples for training or testing purposes in the developed recognition system.

In our system, we employ the Arduino UNO board, which is based on a CMOS 8-bit microcontroller ATmega328 using the RISC architecture and 32k Bytes of in-system programmable flash memory, for walking-step sampling and dynamic walking-pattern recognition. Since the microcontroller ATmega328 can be programmed by employing an integrated development environment (IDE) on a PC, we develop the proposed algorithm for dynamic walking-pattern recognition and uploaded the codes to the microcontroller with a bootloader from the PC via a USB-to-serial converter.

On the other hand, the output voltages from the force sensors are extracted at a sampling rate of 50ms/point as serial discrete voltage points on the Arduino UNO board. The real-time inputted sequential voltage points are mapped to 10-bit resolution (i.e. $0 \sim 1023$ values) and then applied for feature calculation according to the operations, which correspond to our uploaded codes on the microcontroller, generating 8-bit feature results dynamically.

At the initial stage of sample collection for the reference features of the walking steps, the unpredictable walking

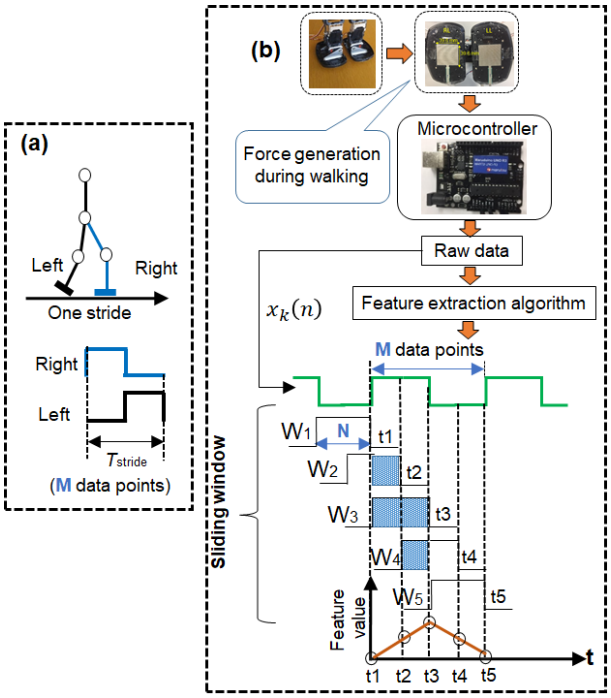

FIGURE 3. (a) One stride walking with sample period T_{stride} represented by M data points; (b) feature extraction procedure basing on the convolution calculation within an overlapped sliding-window method.

status of the robot has to be considered. In order to avoid undesired effects, which can result from mechanical oscillations of the robot, e.g. due to motor vibrations, the data of the first several walking steps of the biped-robot walking on the different types of surfaces are not collected until the robot's walking mode reaches a steady state. When the robot is walking steadily on the different types of surfaces, the generated inertial force-sensory data from the force-sensors are collected in the form of serial input-voltage signals for feature extraction. For the dynamic pattern recognition, we also grant sufficient delay for initialization until the biped robot is walking steadily and then start to activate the real-time recognition stage.

Specifically, one full walking step is considered as one sample period (i.e., one stride), which is denoted by M (M>0) data points (shown in Fig.3a) in our work. So the total time T_{stride} required to cover one sample period is represented as

$$T_{\text{stride}} = M \times T_{\text{sp}}. \tag{1}$$

Here, M is the total number of sampling time points of raw sensory data per walking stride and T_{sp} represents the required time for sampling each point by the microcontroller, as illustrated in Fig.1. Specifically, in our practical experiments, the total sample–point number M of each stride is equal to 76 and our sampling speed is 50 ms per point from the force sensors. Thus, the consumed time for one walking step of the biped robot is approximately equal to $T_{\text{stride}} = 76$ points $\times$ 50 ms/point $= 3.8$ s.

Particularly, the total sample-point number M for each stride depends on the walking speed of the biped robot, which is controlled by changing the number of robot-motor-configuration frames related to the robot-motor design specification. Here, the frame concept includes a certain time unit for adjusting the mechanical parameters of the robot motors, such as a fixed rotation degree. The speed adjustment of the robot walking is realized in terms of a variable frame number for completion of one stride of the biped robot. Specifically, the time-unit interval for one frame in our experiments is equal to 20 ms, i.e., the frame rate is $f_{rate} = 20$ms/frame. Thus the robot walking speed in terms of frame numbers per stride is represented as

$$V_{\text{walking}} = \frac{T_{\text{period}}}{f_{\text{rate}}}. \tag{2}$$

In our experiment, the considered robot-walking speed is 190 frames/stride.

IV. FEATURE EXTRACTION ALGORITHM

Feature selection is the most important step for walking-pattern recognition of the biped robot based on the time-serial force-sensory data. The effect of the feature type on classification performance is even greater than the effect of the classifier type [29]. The random and noisy force-sensory signals are mapped to a feature space for more efficient data processing than possible with the raw-sensory data. Walking-surface identification thus needs an efficient feature-extraction mechanism to figure out the valid sensory-data information for recognizing the target pattern within a noisy environment, reducing information-processing cost and detecting the specific surface-related pattern with high accuracy.

A. TIME-DOMAIN FEATURE DESCRIPTORS

There are various categories of features used in different applications. Approximately, the typical features can be divided into time-domain features, frequency-domain features, special-domain features, etc.

The force sensors used in our system convert the detected robot-feet forces into continuous voltage signals, i.e., analog signals. Since the dynamical analog voltages are sampled by the microcontroller board and transformed into a series of discrete data in the time domain, we naturally prefer to employ time-domain features for dynamic walking-pattern recognition due to the faster calculation without complicated mathematical transformations, which is more suitable for achieving the real-time properties of the proposed system.

Therefore, we have assessed different kinds of time-domain features to find out the most suitable one for dynamic walking-pattern recognition of our biped robot and further integrated all features together as a fused multi-feature descriptor to achieve a much better classification performance. Further, appropriate filtering of high-frequency noise by the feature construction will not only produce better results, but also speed up the pattern-recognition procedure due to the smaller feature-vector size in comparison to the sensor data.

TABLE 1. Feature descriptor and corresponding expression.

No.	Feature Descriptor	Expression
1	RMS	$f_{\mathrm{RMS}}(n) = \sqrt{\frac{1}{N}\sum_{k=1}^{N} x_k^2(n)}$
2	MAV	$f_{\mathrm{MAV}}(n) = \frac{1}{N}\sum_{k=1}^{N} \lvert x_k(n)\rvert$
3	VAR	$f_{\mathrm{VAR}}(n) = \frac{1}{N-1}\sum_{k=1}^{N} x_k^2(n)$
4	MA	$f_{\mathrm{MA}}(n) = \sum_{k=1}^{N-1} \lvert x_{k+1}(n) - x_k(n)\rvert$

Specifically, we have considered the four different time-domain features of Table 1, i.e., root mean square (RMS) [28]–[30], mean absolute value (MAV) [30]–[32], variance (VAR) [30], [32], [33] and mean of amplitude (MA) [29], [30], to extract the necessary information from the raw voltages. Aforementioned feature descriptors are defined by functions as e.g. $f_{\mathrm{RMS}}(n)$ for a time windows of size N ($0<N\leq M$) as shown in Table 1, where n represents a time-window index, denoting the newest sampled data point from the force sensor, which is used for descriptor calculation of this window. The used window concept for the feature descriptors leads to the desired filtering of high-frequency noise. For neighboring windows n and n+1, the relation $x_k(n+1) = x_{k-1}(n)$ between the raw sensor-data points holds for the summations defined in Table 1.

Particularly, the RMS feature descriptor provides the maximum-likelihood estimation of amplitude as Gaussian random process in a constant force and non-fatiguing contraction. MAV is utilized to calculate the moving average of the absolute value of sensory voltages from the force sensors. Variance (VAR) of the sensory voltage is a measure for the average value of the squares of that variable, i.e., it uses the power of the voltage signals in the window for feature construction. The MA feature descriptor, which is also often named waveform length (WL), is the cumulative length of the waveform over the time segment of the serial sensory data. MA combines the measurement of waveform amplitude, frequency and duration time, describing the sensory signal complexity.

The results obtained with the above four feature descriptors for the continuous voltage signals from the force sensors during robot walking are presented and discussed in section VI.

B. FEATURE EXTRACTION USING A SLIDING- WINDOW STRATEGY

Streaming of input data allows calculating the feature vectors in a stepwise manner. The sliding window technique has been introduced as such a stepwise manner for time segmentation of raw input data in [24] and [29], aiming at real-time processing. The former technique [24] sampled streaming features in real-time by a size-adaption of the sliding window. Reference [29] discussed performance differences of the adjacent-window and the overlapped-window approaches, using a surface electromyography (sEMG) control system. In our implementation, we have considered the overlapped-window approach because it uses the available time to process more data, so that as a result the classification accuracy becomes higher than with the adjacent-window approach [25]–[27].

For dynamic walking-pattern recognition, we utilize moving-time windows of fixed-size N ($0<N\leq M$) to process the streaming voltages from the force sensors, mounted under the feet of the biped robot, for real-time feature extraction and fast walking-pattern recognition. As illustrated in Fig. 3, the dynamic N-point window is used to slide over the serial-input force-sensor data when the biped robot is walking at a certain speed with a stride of M discrete-time points inputted by the microcontroller. The streaming feature vectors, according to the feature descriptors illustrated in Table 1, are sampled step-by-step with the dynamic sliding window, overlapping on the discrete sequential sensory data $x_k(n)$, $k\in[1, 2, \ldots, N]$. The feature-extraction procedure is equivalent to the convolution calculation between the discrete time-series sensory voltages $x_k(n)$ and the N-point window, using a weight-factor of magnitude '1'.

Figure 3 (b) illustrates an ideal case of the discrete time-linear convolution procedure for feature generation during one stride of ideal sensory data and a sliding window of size N, where N=M/2. We show how raw sensor data and sliding-window function are convoluted with each other to generate features dynamically at five different time instances.

- Time t_1: Raw sensor data in overlap region with sliding window is zero. Thus, the feature value becomes zero.
- Time t_2: Raw sensor data is positive in part of the sliding window. As a result, the feature value is increasing.
- Time t_3: Raw sensor data is positive in complete sliding window, so that the feature value increase to its maximum.
- Time t_4: Raw sensor data is again positive in only part of the sliding window. As a result, the feature value is decreasing.
- Time t_5: Raw sensor data is again zero in sliding window. As a result, the feature value returns to zero.

By combining all feature values at different time instances from t_1 to t_5, a triangular wave form is generated for each descriptor respectively (see Fig.3 (b)).

The RMS-feature descriptor is employed as an example to illustrate the generation procedure of feature values from the measured force-sensor data (of the right foot), using a dynamic window to slide over the sequential discrete sensory voltages $x_k(n)$, as illustrated in Fig. 4. During the dynamic walking process of the biped robot, the current RMS feature vector is generated in terms of the convolution results of raw sensory data within the range of the current window. Along with the window shifting, the oldest raw sensory point in the previous window is discarded and the newly inputted sensory value is included in the range of next shifted window. Each point of the blue curve, i.e., the feature vector, represents the convoluted value of the sliding window and raw sensor data with RMS feature descriptor. In Fig. 4, we have highlighted five different RMS-feature points with pink circles and indicated also the corresponding sliding windows. To improve the

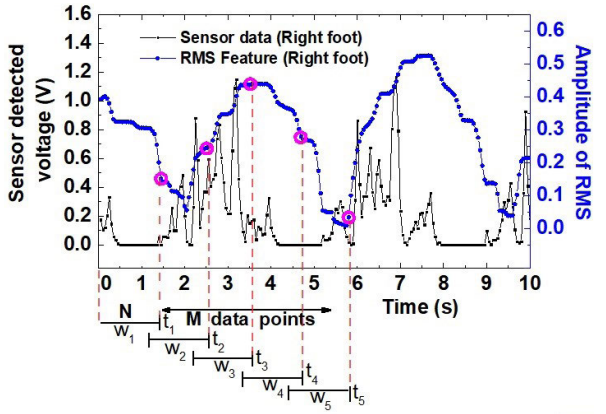

FIGURE 4. Real-time feature extraction using a sliding-window algorithm with fixed window size N (0<N≤M, M represents the total number of sampling time points of raw sensory data per walking stride).

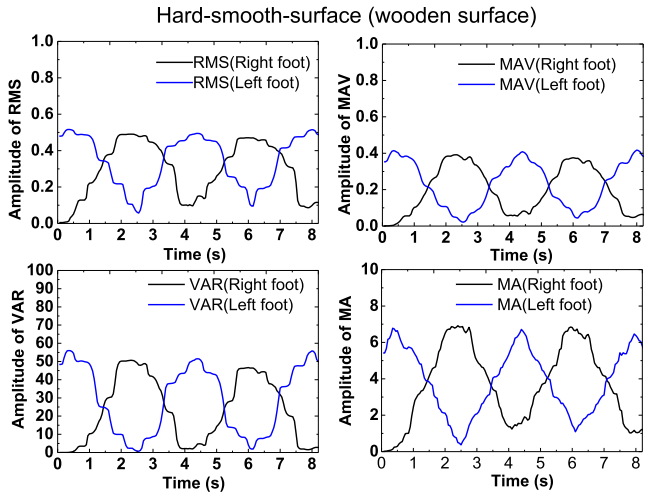

FIGURE 5. Force-sensor-extracted dynamic-walking features (RMS, MAV, VAR and MA) for left and right foot on a hard-smooth surface (wooden surface) with 50ms sampling rate.

responding speed for fast recognition with lower-dimensional feature vectors, we employed a sliding window with a fixed size of N=M/2 (50% of stride duration), i.e., N=38, with 38×50 ms=1.9 s duration for each window.

The feature properties corresponding to the four chosen feature descriptors, i.e., RMS, MAV, VAR, and MA, are different from each other while calculated with the same serial input of raw sensory data from the same surface, such as a hard-smooth-surface (wooden table) as shown in Fig. 5.

When the robot feet touch the surface, the relative changes in feature amplitudes of RMS, MAV, and MA are smaller than those of the VAR feature due to the square calculation in the corresponding equation, as listed in Table 1. Further, the calculated features are more distinctive from each other when compared to the raw sensory data.

Note that it is not necessary to use all time points of one stride for feature extraction to achieve fast walking-pattern recognition of the biped robot, because the raw sensory data usually show lots of redundancy and noise that should be removed.

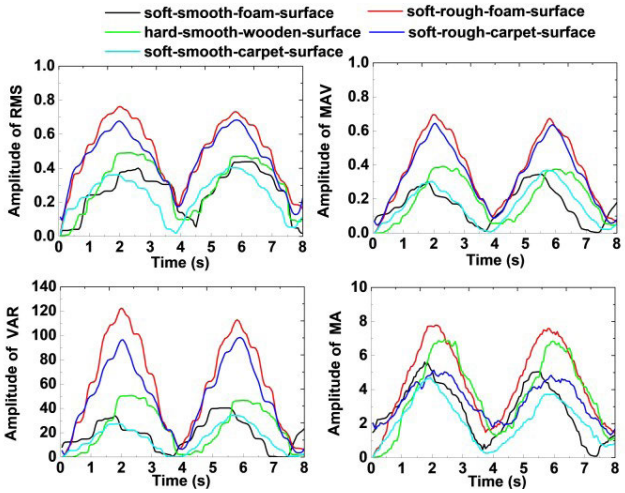

FIGURE 6. Force sensor extracted dynamic walking features (RMS, MAV, VAR and MA) for the right foot using five different surfaces (black: soft-smooth-foam-surface, red: soft-rough-foam-surface, green: hard-smooth-surface (wooden surface), blue: soft-rough-surface (carpet), sky-blue: soft-smooth-thin-surface (thin carpet)).

C. FEATURE EXTRACTION ON DIFFERENT SURFACES

To obtain corresponding tactile properties of the force sensor touching on five flat surfaces in the human living environment, as shown in Fig.2, we have extracted the feature vectors using the four different descriptors listed in Table 1, respectively, employing the aforementioned feature generation method with the sliding-window strategy.

We quantitatively evaluated the impact of tactile properties such as roughness and hardness of different surfaces on the force sensors, which are mounted under the two feet of the biped robot, during walking. As indicated in Fig.6, amplitude and shape of the feature curves, generated for each surface with the same descriptor, are distinguishable from each other due to the different friction and contact forces between the sensors and the surfaces. Further, the feature curves of the four feature descriptors obtained for the same surface are distinctive from each other as well. Thus, we have applied these four feature descriptors to generate the real-time feature vectors for on-line walking-pattern recognition of the biped robot on different surfaces in this work.

The performance of each kind of feature descriptor for walking-pattern recognition has been verified and a way to integrate these four feature descriptors to maximize the classification performance for the multi-surface recognition by the biped robot has been investigated.

V. ON-LINE WALKING-PATTERN RECOGNITION

Surface identification is based in this work on analyzing the walking patterns in terms of the dynamic sensory data inputted from the force sensors mounted under the feet of the biped robot. For dynamic pattern recognition through online usage of the resource-limited microcontroller, we trained the stride reference-samples offline and designed discrete classes per surface type, i.e., for the walking pattern of the biped robot on this surface, enabling the classification of the sensors'

force characteristics during robot walking on the corresponding surfaces.

The Euclidean distance is used as in (3) for the distance metric of the k-nearest neighbor (kNN) classifier in our on-line matching algorithm, which compares the feature vectors $FV_{in}(i)$ extracted from the real-time input-sensory data to features vectors $FV_{ref}(i)$ from the selected walking-pattern-reference data corresponding to each of the surfaces.

$$\text{Dist} = \sqrt{\sum_{i=1}^{d} \left(FV_{ref}(i) - FV_{in}(i)\right)^2} \tag{3}$$

Both, real-time input feature vector $FV_{in}(i)$ and reference feature vector $FV_{ref}(i)$ in (3) are calculated according to the feature descriptors listed in Table 1. The dimensionality d of feature vectors, i.e., the feature length, for accumulating the distance is selected within the number of data points for one stride. Similar to the sliding-window strategy, applied to feature extraction in Section IV.B, it is unnecessary to utilize all data values in one period of the feature for pattern recognition. Thus, we employ the feature length (or dimension) of d=20 points for fast distance calculation according to (3).

The kNN classifier finds the nearest k reference patterns to the input pattern and determines the finally recognized class for this input pattern according to the class with the maximum number of representations among the nearest k reference patterns [35]–[37]. The kNN classifier is widely used for binary classifications as well as for all the possible combinations between pairs of classes in multiple-class problems. Such a one-versus-one (OVO) scheme is normally applied to distinguish a positive category from a negative category. Real application scenarios of a human living environment generally involve more than two kinds of walking surfaces. In other words, the robot has to recognize the transit between multiple surfaces, which leads to a multi-class problem.

For solving a multi-class problem, a previous approach [38] proposed a multi-label strategy to represent a single instance with a set of labels simultaneously, while considering the correlations between different labels. However, the multi-class problem in this work is different from [38], because the employed classifier has to distinguish the given walking surface from all other walking surfaces, i.e., requires a one-versus-all (OVA) scheme. Besides, each surface (class) is represented by a single label and has practically no correlation to the other surfaces.

All in all, during the online walking-pattern recognition of the biped robot in our work, the correct pattern of the real-time input-sensory data has to be detected and matched to one of the given reference classes (surfaces) in real time. For the on-line walking-pattern recognition in our system, we labeled one reference pattern for each walking surface. In addition, only k=1 is employed in the online kNN recognition model for reducing the processing time. Thus, the reference pattern having the minimum Euclidean distance from the input walking pattern is considered to determined output class for this input pattern. Figure 7 shows our on-line recognition system

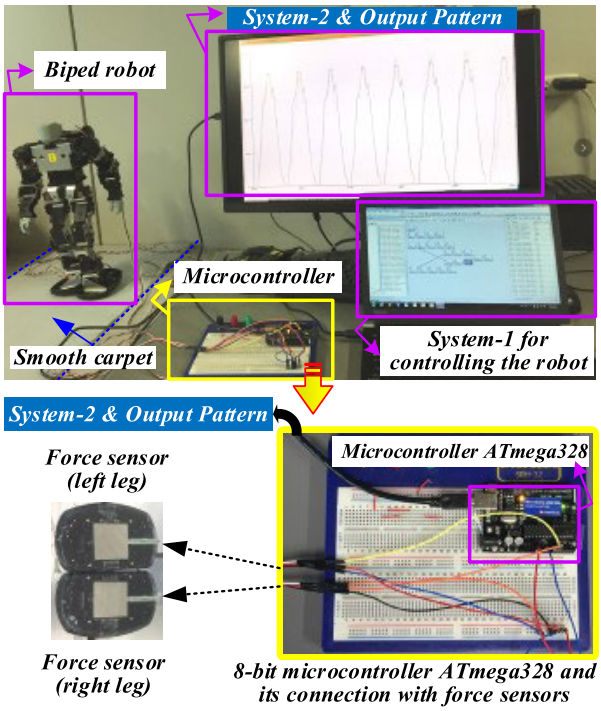

FIGURE 7. Proposed on-line walking-pattern recognition system.

for robot walking patterns with nearly instant recognition results.

Note that there is no need to store the real-time input sensory data for on-line pattern recognition in the on-board memory since the sensory data are processed immediately by the uploaded code on the microcontroller, once they are inputted from the force sensors, and the calculation results are instantly transferred to the PC terminal and shown in the data monitor.

VI. EXPERIMENTAL RESULTS AND MODEL ANALYSIS

To evaluate the performance of biped-robot walking-pattern recognition by the proposed recognition model using the k-nearest neighbor (kNN) algorithm as the classifier, we collected 300 robot strides of force-sensory data per surfaces at a walking speed of 3.8 seconds/stride for training, and another 200 robot strides per surfaces for testing. Each stride, consisting of M=76 force-sensor-data points per robot foot, is considered as a walking-pattern sample in training dataset or testing dataset.

The constant value of k in the kNN classifier can influence the accuracy of the overall classification. In reality, the value of k is usually an odd number. We tested the classification results with six different k values, i.e., k=1, 3, 5, 7, 9, 11. As a machine learning task, the walking patterns corresponding to the five surfaces, listed in Fig.2, are labeled to the corresponding class, respectively.

First of all, we measured the four different feature descriptors (i.e., MAV, VAR, RMS, MA listed in Table 1) independently with the binary kNN classifier on five respective walking surfaces using the OVO scheme, to find out the

separate impact of each feature descriptor on the walking-pattern recognition of the biped robot.

Given the variety of walking surfaces in real-world environments, a real multi-class recognition model is further built up and evaluated based on the OVA scheme. Further, we integrated the four features into a fused multi-feature descriptor for the multi-class problem, to optimize the classification performance of the OVA scheme, so that a sufficient prediction rate can be achieved for an unknown input surface (i.e., an unlabeled input pattern) with multiple possibilities for the real application scenario.

A. BINARY CLASSIFICATION

First of all, we have thus formulated a simplified binary classification problem for distinguishing the positive surface (i.e., the target object) from different negative surfaces independently when the biped robot is walking in the human living environment. For verifying the classification accuracy (ACC) as in (4) and precision (PRE) as in (5) on different walking surfaces, we trained the force-sensory data extracted from the hard-smooth surface (wooden table) as the positive samples, while the four other kinds of force-sensory data from the soft-smooth surface (smooth foam), the soft-rough surface (rough foam), the soft-rough surface (carpet), and the soft-smooth thin surface (thin carpet) were labeled as negative samples, respectively.

$$\mathrm{ACC} = \frac{\mathrm{TP}+\mathrm{TN}}{\mathrm{P}+\mathrm{N}} \times 100\% \tag{4}$$

$$\mathrm{PRE} = \frac{\mathrm{TP}}{\mathrm{TP}+\mathrm{FP}} \times 100\% \tag{5}$$

Here, P is the number of all positive samples, N represents the number of negative samples, TP is the number of true positive samples (i.e., positive samples detected correctly among all positive samples), TN represents the number of true negative samples (i.e., negative samples correctly detected among all negative samples), and FP is the number of false positive samples (i.e., positive samples detected incorrectly among all negative samples).

One example of the OVO binary classification model, employing the hard-smooth surface as positive samples and the other four surfaces as negative samples, is built up. Then, its classification performances in the above four cases with the kNN classifier (k=3) are determined and the accuracy results are plotted in Fig.8. Specifically, all cases are tested with P=100 positive samples on hard-smooth surface, and N=100 negative samples corresponding to one of the other four walking surfaces respectively. Before the testing procedure, 150 positive samples and 150 negative samples for each surface case, evaluated in Fig.8, were labeled and trained in advance. Each sample in training dataset or testing dataset consists of M=76 force-sensor-data points per stride of the biped robot.

We measured the impact on recognition performance of the aforementioned four feature descriptors independently in combination with the kNN classifier. Each feature descriptor

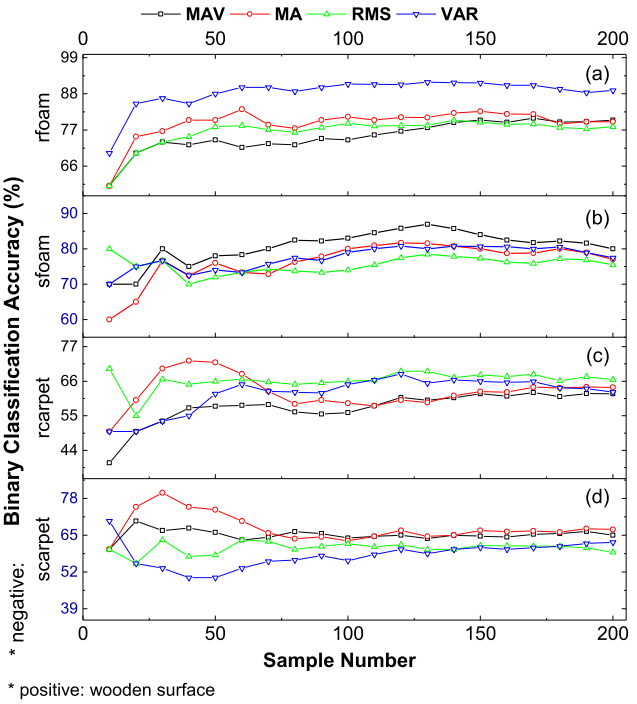

FIGURE 8. Binary classification accuracy using four different feature descriptors and the k-NN classifier (k=3), for recognizing the positive samples (hard-smooth surface) against 4 different negative samples independently, i.e., (a) the rough foam (rfoam), (b) the smooth foam (sfoam), (c) the rough carpet (rcarpet), and (d) the smooth carpet (scarpet).

seems to have its merits with respect to different negative surfaces. In the case of using the rough foam surface as the negative surface, the VAR feature descriptor is found to achieve the highest maximum accuracy 91.54% (k=3) in comparison to the other three descriptors, as listed in Table 2. In the case of using the smooth foam surface as negative surface, the MA feature descriptor achieves the highest accuracy of 90 % (k=9).

However, the accuracy maxima for all four types of feature descriptors MAV, RMS, VAR, and MA decline in the cases where smooth-carpet or rough-carpet results are used for the negative reference samples. The main reason for classification-performance degradation using these two surfaces for the negative reference samples lies most likely in a higher similarity of the robot's walking pattern when the walking surface has higher similarity to the smooth-wood surface.

B. MULTI-CLASS MODEL ANALYSIS

In order to classify input samples in real-world applications with multiple classes, a one-versus-all (OVA) approach is often used. In this section, we evaluate the performance of the kNN classification model with OVA approach and five classes, representing the selected test surfaces, for the surface recognition task based on the walking pattern of the biped robot.

With 150 training-set samples and 25 testing-set samples, extracted for each of the separate surfaces exhibited in Fig.2,

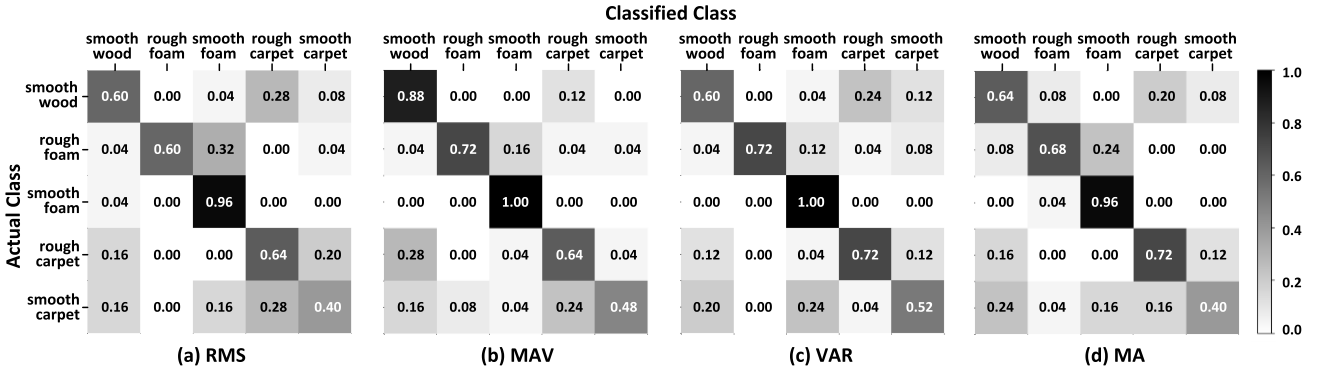

FIGURE 9. Confusion matrices for recognition rate of the 5 different surfaces, based on the OVA scheme with 4 separate feature descriptors (RMS, MAV, VAR, MA). Rows indicate the actual testing surface, while the columns indicate the corresponding surface classes recognized. The numbers give the obtained OVA classification rates. The k (k<12) corresponding to the maximum recognition rate was chosen for the kNN Algorithm.

TABLE 2. Maximum binary kNN classification accuracy.

Positive Sample	Negative Sample	Feature Descriptor	Maximum Binary Accuracy (%) *					
			k=1	k=3	k=5	k=7	k=9	k=11
Smooth Wood	Smooth Foam	MAV	**86.92**	**86.92**	86.15	86.15	86.15	**86.92**
		RMS	75.00	80.00	**83.85**	83.57	83.08	83.57
		VAR	78.00	80.83	83.33	85.83	**86.67**	**86.67**
		MA	83.33	81.67	86.67	89.23	**90.00**	87.69
	Rough Foam	MAV	**85.00**	80.59	82.94	83.57	83.53	84.71
		RMS	**88.33**	80.00	83.33	81.43	81.43	80.71
		VAR	91.43	**91.54**	89.33	88.67	88.67	88.67
		MA	82.5	83.33	84.00	84.67	86.67	**87.33**
	Smooth Carpet	MAV	70.00	70.00	71.11	71.11	**72.11**	71.05
		RMS	64.21	63.33	65.72	**80.00**	70.00	66.67
		VAR	60.53	70.00	**80.00**	**80.00**	70.00	70.00
		MA	76.67	**80.00**	**80.00**	70.00	65.00	68.33
	Rough Carpet	MAV	62.50	62.35	61.58	62.94	65.00	**67.50**
		RMS	67.06	**70.00**	66.47	65.00	65.79	65.29
		VAR	62.50	**68.33**	62.94	64.12	66.47	65.88
		MA	**70.00**	72.50	65.29	65.88	63.33	66.00

* Window Size=1/2 stride, Left foot of the biped robot.

the performance of the kNN model (k=1, 3, 5, 7, 9, 11) based on the OVA scheme is estimated with the aforementioned features independently. The experimental classification performances for the five surfaces are evaluated and exhibited in the confusion matrices of Fig.9. A confusion matrix gives a visualization of the classification sensitivity of the feature descriptors through the proportional classification distribution $p_{i,j}$ over all classes j with respect to test samples from each actual input class i (i.e., walking surface). In particular, each row i of the confusion matrix lists, therefore, the classification distribution of one actual testing class over all possible output classes.

The maximum proportion $p_{i,j}$ $(i = j)$ in the diagonal line of the confusion matrix can be considered as the recall (i.e., true positive rate) of our OVA classification model as well. The four feature descriptors RMS, MAV, VAR, and MA have been used independently for the classification in this section. The OVA classification model achieved the highest recall rates for the smooth-foam-surface data with all four feature descriptors (RMS: 96%, MA: 96%, MAV: 100%, VAR: 100%), while the smooth-carpet surface is the most easily misclassified surface among all other surfaces, resulting from similarities in rigidity and smoothness when compared to the rough-carpet and smooth-wood surfaces. Unfortunately, the multi-classification accuracies of all investigated feature descriptors (RMS: 64%, MAV: 74.4%, VAR: 71.2%, MA: 68%) are still unsatisfactory when employing the OVA strategy. The walking-pattern recognition on diverse surfaces gets increasingly challenging, if the number of involved surfaces is increased, as the recognition model must distinguish more types of walking patterns correctly. Besides, the vibration-based surface-recognition models, employing force sensors mounted under the biped-robot feet, perform worse on the different surfaces fabricated with similar materials.

C. FEATURE COMBINATION PERFORMANCE ANALYSIS

To improve the classification performance in the multi-class recognition model, we combine the advantages of all four separate kNN classifiers, each using one of the four independent feature descriptors.

First of all, the true positive rate (i.e., recall) of one given set of labeled testing samples in our OVA scheme is calculated by the combination classification results of four feature descriptors as in (6)

$$p_{\text{pos,COM}} = {TP_{\text{COM}}}/{P}, \tag{6}$$

where TP_{COM}, P and $p_{\text{pos,COM}}$ refer to the number of true-positive-classified samples of the combined classification, the total number of positive samples and the combined positive rate, respectively. According to the above combination equation, the current testing sample is classified into the class for which at least one of the four kNN classifiers confirms it as a positive sample, i.e., $TP_{\text{COM}} = TP_{RMS} \cup TP_{MAV} \cup TP_{VAR} \cup TP_{MA}$.

Otherwise, we check whether a majority of the four classifiers gives the same class as the classification result and

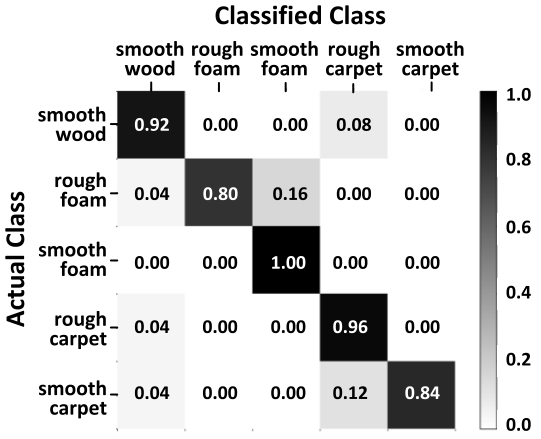

FIGURE 10. Confusion matrix performed with OVA scheme, which combines the kNN (k=3) classifier with an integrated feature descriptor, combining RMA, MAV, VAR and MA descriptors, for the classification of the biped-robot walking pattern on the 5 different surfaces.

assign this class (i.e. the corresponding walking surface) to the testing sample. If a majority decision is not possible, the assigned class is determined randomly among the classes with equal classification counts from the four kNN classifiers based on different feature descriptors.

The proportional classification distribution $p_{i,j}$ of the confusion matrix of the OVA scheme, employing the combined feature descriptor, is exhibited in Fig. 10. The model performance for each surface is measured using 25 stride samples in this experiment. The combined recalls of each testing surfaces are significantly improved (table: 92%; rough foam: 80%; smooth foam: 100%; rough carpet: 96%; smooth carpet: 84%), when compared to the solutions with each individual feature descriptor. The diagonal values of the confusion matrix are much higher than the off-diagonal values for the other surfaces in each row, so that the combined feature-descriptor model distinguishes the correct surface from other negative surfaces more easily, due to the higher sensitivity.

Further, the combined-feature OVA classification model achieves about 90.4% overall accuracy for solving the multi-class problem among C classes (C=5 in this work) according to (7).

$$ACC_{multi} = \frac{1}{C}\sum_{i=1}^{C} p_{i,i} \tag{7}$$

The precisions of the combined feature descriptor for recognizing the walking pattern of the biped robot on each surface is also significantly improved when comparing to each individual feature descriptor, as listed in Table 3, resulting in table: 88.46%, rough foam: 100%, smooth foam: 86.21%, rough carpet: 82.76%, and smooth carpet: 100%. The average precision of the multi-class model reaches therefore 91.49%.

D. COMPARISON WITH OTHER WORK

Diversified intelligent-robot systems have been developed in the resent decade for various purposes and industrial applications. In this section, we present a comparative analysis of six different types of approaches, using different robot

TABLE 3. Classification prescision comparison.

Feature Descriptor	Precision (%)				
	Smooth Wood	Rough Foam	Smooth Foam	Rough Carpet	Smooth Carpet
RMS	60.00	100	64.86	53.33	55.56
MAV	64.71	90.00	80.65	61.54	85.71
VAR	60.00	100	66.67	66.67	59.09
MA	57.14	80.95	70.59	66.67	66.67
Combined	**88.46**	**100**	**86.21**	**82.76**	**100**

systems, with our proposed implementation for real-time surface identification. Although it is hard to evaluate and compare the performance of different intelligent-robot systems by using a single criterion, we list the critical elements of the respective approaches and their corresponding results in Table 4.

Particularly, the reported work in [3] investigated a ground-surface-pattern identification for navigation by using tactile probes built and fitted on a wheeled robot with differential drive. It was demonstrated that the variance (VAR) feature performed better as an indicator of the movement pattern than nine other analyzed time-domain features, a result which is similar to our work. Comparable classification-accuracy rates of 89.9%±0.4% with a 1-second time window and 99.96±0.02% with 4-second time window could be achieved when employing a more complicated artificial-neural network (ANN) as the classifier in [3]. However, the ANN method resulted in much higher computational cost than our approach. Besides, a sharp classification-accuracy decline to 74.1% occurred, when an unsupervised-learning classifier was used.

Surface detection using the quadruped Sony AIBO robot with three kinds of sensors, i.e., accelerometer, infrared range sensor, and ground-contact-force sensor, was reported in [4]. The random-forests classifier was found to be most accurate among nine examined classifiers, achieving 94% accuracy for domestic environments. However, the random-forests classifier was also found to be very time- and resource- consuming. The smaller forest classifier still consumed 833 kB RAM and showed declined accuracy of 90.9% in [4]. Reference [5] proposed a recognition framework, which combined the Unevenness Point Descriptor (UPD) for feature extraction with the SVM classifier for surface detection, using a hexapod robot and three cost-effective sensors (F/T sensor, depth, and vision). The feature vector was extended by calculating the FFT of the acquired signals. Maximum precision 94.44% was achieved for 12 classes of different terrains.

For the surface classification, approach [6] used the AdaBoost classifier to classify convex-type surfaces with a low-cost force sensor, which is similar to our used force-sensor approach. Hoepflinger *et al.* [6] sampled the sensor data at 50 Hz frequency for the classification of four different surfaces. Each surface was based on 25 training samples and 15 testing samples. Approximately 93.3% accuracy rate was

TABLE 4. Comparison with other state-of-the-art works.

Approach	Feature	Classifier	Sensors	Types of robot	Sampling Rate	Performance
[3]	VAR, etc. (8 types)	ANN	Tactile probe (a metallic rod with a solid-state accelerometer)	Wheel robot (mobile robot)	4 kHz	> 89.9% (accuracy)
		Unsupervised Learning				74.1% (accuracy)
[4]	FFT	kNN, SVM, Random Forest, etc. (9 types)	Accelerometer, infrared range sensor & ground contact force sensor	Quadruped robot	120 Hz (accelerometer); 25 Hz (infrared range) 10Hz (force sensor)	91% ~ 94% (accuracy)
[5]	UPD	SVM	Vision, depth & force-torque sensor	Hexapod robot	200 Hz	94.44% (precision)
[6]	Mean, etc. (5 types)	AdaBoost	Force/torque sensor	Quadruped robot	50 Hz	94% (accuracy)
[13]	DWT & FFT	SVM	Force/torque sensor	Humanoid robot	100 Hz	95.16±0.8% (mean precision)
[34]	Peak, etc. (16 types)	SMO-based SVM	Capacitive tactile sensor	Biped robot	~260 Hz	> 90% (accuracy)
This work	VAR, etc. (4 types)	kNN	Force sensor	Humanoid robot	20 Hz	90.4% (accuracy) 91.5% (average precision)

achieved for surface classification based on sensor data from a single leg in [6]. Another similar research work [13] was reported for terrain-surface classification with a humanoid robot. Approximately 94.23% and 93.33% precision were achieved using a FFT and a DWT descriptor, respectively. The SVM classifier was applied for recognition of a wood-surface terrain.

Ground-reaction-force (GRF) sensing and surface classification, using a curved-feet-based biped robot with a surface-mounted capacitive tactile sensor, was reported in [34]. The presented terrain-classifier performance was measured on the MATLAB profiler, using the SVM classifier to detect six different types of surfaces with > 90% accuracy. However, the reported method suffers from a hysteresis problem during long-time usage.

In this paper, we used the kNN classifier combined with four kinds of feature descriptors to estimate the performance of walking-pattern recognition for a biped robot on five types of surfaces. An overall accuracy of 90.4% was achieved by applying a simple and flexible recognition system with low-cost force sensors. The recognition-model precision on rough-foam and smooth-carpet surfaces can reach both 100% when using the combined feature descriptor and the kNN classifier, where we considered k=3 and a 1/2 -stride sliding-window. In this case an average-precision result of 91.49% was also obtained with the studied five walking surfaces. The proposed on-line surface-detection system can operate without storage of intermediate computational data and can be implemented on a low-cost microcontroller with limited resources of 32 kB flash memory. The applied sliding-window method has the advantage of requiring much less memory and processing speed because its computational operation and memory access only occur once in a particular time instant.

Note that the surface detection is done in our work with force sensors at the sampling rate of 20Hz, which is lower in comparison to other works, due to the limitations by the employed low-level microcontroller. If necessary, the sampling rate in our proposed system could, of course, be increased easily by employing a higher-performance microcontroller.

VII. CONCLUSION

In this work, we explored how to distinguish the strides of a small humanoid robot on different surfaces by recognizing the corresponding walking patterns, represented by the force sensory data, so as to adjust the postures of the biped robot and give the robot the capability of being more natural and stable during walking on different ground surfaces, similar to human beings. A sliding-window algorithm is used to generate four different types of dynamic features and the k-nearest neighbor (kNN) classifier is used to recognize the multiple types of surfaces.

Given the multi-class problem, we measured and compared the performance of a binary model and a multi-class model for the walking-pattern recognition of the biped robot on five different surfaces. Besides, we combined the analyzed four feature descriptors MAV, RMS, VAR, and MA into a fused feature descriptor, where our analysis results show 90.4% maximum classification accuracy and 91.49% average precision. This verifies the realization of a better cost-performance trade-off than in other previous research works. The analysis result of our proposed work is useful for future AI-based robot-system design, where the robot can balance by itself by changing its joint-motor angles in accordance with the recognized different types of surfaces.

REFERENCES

[1] C. A. Brooks and K. Iagnemma, "Vibration-based Terrain classification for planetary exploration rovers," *IEEE Trans. Robot.*, vol. 21, no. 6, pp. 1185–1191, Dec. 2005.
[2] C. Weiss, H. Frohlich, and A. Zell, "Vibration-based terrain classification using support vector machines," in *Proc. Int. Conf. Intell. Robots Syst. (IEEE/RSJ)*, Beijing, China, Oct. 2006, pp. 4429–4434.
[3] P. Giguere and G. Dudek, "A simple tactile probe for surface identification by mobile robots," *IEEE Trans. Robot.*, vol. 27, no. 3, pp. 534–544, Jun. 2011.
[4] C. Kertész, "Rigidity-based surface recognition for a domestic legged robot," *IEEE Robot. Autom. Lett.*, vol. 1, no. 1, pp. 309–315, Jan. 2016.
[5] K. Walas, "Terrain classification and negotiation with a walking robot," *J. Intell. Robotic Syst.*, vol. 78, nos. 3–4, pp. 401–423, 2015.

[6] M. A. Hoepflinger, C. D. Remy, M. Hutter, L. Spinello, and R. Siegwart, "Haptic terrain classification for legged robots," in *Proc. Int. Conf. Robot. Autom.*, Anchorage, AK, USA, May 2010, pp. 2828–2833.
[7] C. Kertész, "Exploring surface detection for a quadruped robot in households," presented at the 14th IEEE Int. Conf. Auton. Robot Syst. Competitions, Espinho, Portugal, May 2014.
[8] S. T. Namin and L. Petersson, "Classification of materials in natural scenes using multi-spectral images," in *Proc. IEEE/RSJ Int. Conf. Intell. Robots Syst.*, Vilamoura, Portugal, Oct. 2012, pp. 1393–1398.
[9] K. Walas and M. Nowicki, "Terrain classification using laser range finder," in *Proc. IEEE/RSJ Int. Conf. Intell. Robots Syst.*, Chicago, IL, USA, Sep. 2014, pp. 5003–5009.
[10] A. Chemori, S. Le Floch, S. Krut, and E. Dombre, "A control architecture with stabilizer for 3D stable dynamic walking of SHERPA biped robot on compliant ground," in *Proc. 10th IEEE-RAS Int. Conf. Humanoid Robots*, Nashville, TN, USA, Dec. 2010, pp. 480–485.
[11] L. C. Visser, S. Stramigioli, and R. Carloni, "Control strategy for energy-efficient bipedal walking with variable leg stiffness," in *Proc. IEEE Int. Conf. Robot. Automat.*, Karlsruhe, Germany, May 2013, pp. 5624–5629.
[12] Y. Takahashi, K. Nishiwaki, S. Kagami, H. Mizoguchi, and H. Inoue, "High-speed pressure sensor grid for humanoid robot foot," in *Proc. IEEE/RSJ IEEE Int. Conf. Intell. Robots Syst.*, Edmonton, AB, Canada, Aug. 2005, pp. 3909–3914.
[13] K. Walas, D. Kanoulas, and P. Kryczka, "Terrain classification and locomotion parameters adaptation for humanoid robots using force/torque sensing," in *Proc. 16th IEEE-RAS Int. Conf. Humanoid Robots*, Cancun, Mexico, Nov. 2016, pp. 133–140.
[14] Y.-L. Park, B.-R. Chen, and R. J. Wood, "Design and fabrication of soft artificial skin using embedded microchannels and liquid conductors," *IEEE Sensors J.*, vol. 12, no. 8, pp. 2711–2718, Aug. 2012.
[15] S. Harada, K. Kanao, Y. Yamamoto, T. Arie, S. Akita, and K. Takei, "Fully printed flexible fingerprint-like three-axis tactile and slip force and temperature sensors for artificial skin," *ACS Nano*, vol. 8, no. 12, pp. 12851–12857, 2014.
[16] J. B. Gafford, S. B. Kesner, A. Degirmenci, R. J. Wood, R. D. Howe, and C. J. Walsh, "A monolithic approach to fabricating low-cost, millimeter-scale multi-axis force sensors for minimally-invasive surgery," in *Proc. IEEE Int. Conf. Robot. Autom.*, Hong Kong, May/Jun. 2014, pp. 1419–1425.
[17] A. Shashank, M. I. Tiwana, S. J. Redmond, and N. H. Lovell, "Design, simulation and fabrication of a low cost capacitive tactile shear sensor for a robotic hand," in *Proc. IEEE EMBC*, Minneapolis, MN, USA, Sep. 2009, pp. 4132–4135.
[18] A. Schmitz, P. Maiolino, M. Maggiali, L. Natale, G. Cannata, and G. Metta, "Methods and technologies for the implementation of large-scale robot tactile sensors," *IEEE Trans. Robot.*, vol. 27, no. 3, pp. 389–400, Jun. 2011.
[19] S. Takenawa, "A magnetic type tactile sensor using a two-dimensional array of inductors," in *Proc. IEEE Int. Conf. Robot. Autom.*, Kobe, Japan, May 2009, pp. 3295–3300.
[20] J.-I. Yuji and S. Shiraki, "Magnetic tactile sensing method with Hall element for artificial finger," in *Proc. 7th Int. Conf. Sens. Technol.*, Wellington, New Zealand, Dec. 2013, pp. 311–315.
[21] M. Hoffmann, K. Štepánová, and M. Reinstein, "The effect of motor action and different sensory modalities on terrain classification in a quadruped robot running with multiple gaits," *Robot. Auton. Syst.*, vol. 62, no. 12, pp. 1790–1798, Dec. 2014.
[22] Kondo Kagaku Co. *Specification of KHR-3HV Ver.2 Robot*. Accessed: Dec. 20, 2018. [Online]. Available: https://kondo-robot.com/product/03178
[23] Taiwan Alpha Electronic Co. *Specification of Membrane Force Sensors Provided by Alpha*. Accessed: Apr. 10, 2019. [Online]. Available: http://www.taiwanalpha.com/en/products/21
[24] D. You, X. Wu, L. Shen, S. Deng, Z. Chen, C. Ma, and Q. Lian, "Online feature selection for streaming features using self-adaption sliding-window sampling," *IEEE Access*, vol. 7, pp. 16088–16100, 2019.
[25] M. A. Oskoei and H. Hu, "Myoelectric control systems—A survey," *Biomed. Signal Process. Control*, vol. 2, no. 4, pp. 275–294, Oct. 2007.
[26] T. R. Farrell, "Determining delay created by multifunctional prosthesis controllers," *J. Rehabil. Res. Dev.*, vol. 48, no. 6, p. 6, 2011.
[27] K. Englehart and B. Hudgins, "A robust, real-time control scheme for multifunction myoelectric control," *IEEE Trans. Biomed. Eng.*, vol. 50, no. 7, pp. 848–854, Jul. 2003.
[28] T. R. Farrell and R. F. F. Weir, "A comparison of the effects of electrode implantation and targeting on pattern classification accuracy for prosthesis control," *IEEE Trans. Biomed. Eng.*, vol. 55, no. 9, pp. 2198–2211, Sep. 2008.
[29] M. Hakonen, H. Piitulainen, and A. Visala, "Current state of digital signal processing in myoelectric interfaces and related applications," *Biomed. Signal Process. Control*, vol. 18, pp. 334–359, Apr. 2015.
[30] X. Xi, M. Tang, S. M. Miran, and Z. Luo, "Evaluation of feature extraction and recognition for activity monitoring and fall detection based on wearable sEMG sensors," *Sensors*, vol. 17, no. 6, p. 1229, May 2017.
[31] B. Hudgins, P. Parker, and R. N. Scott, "A new strategy for multifunction myoelectric control," *IEEE Trans. Biomed. Eng.*, vol. 40, no. 1, pp. 82–94, Jan. 1993.
[32] M. Zardoshti-Kermani, B. C. Wheeler, K. Badie, and R. M. Hashemi, "EMG feature evaluation for movement control of upper extremity prostheses," *IEEE Trans. Rehabil. Eng.*, vol. 3, no. 4, pp. 324–333, Dec. 1995.
[33] S.-H. Park and S.-P. Lee, "EMG pattern recognition based on artificial intelligence techniques," *IEEE Trans. Rehabil. Eng.*, vol. 6, no. 4, pp. 400–405, Dec. 1998.
[34] X. A. Wu, T. M. Huh, R. Mukherjee, and M. Cutkosky, "Integrated ground reaction force sensing and terrain classification for small legged robots," *IEEE Robot. Autom. Lett.*, vol. 1, no. 2, pp. 1125–1132, Jul. 2016.
[35] M. T. Hoang, Y. Zhu, B. Yuen, T. Reese, X. Dong, T. Lu, R. Westendorp, and M. Xie, "A soft range limited K-nearest neighbors algorithm for indoor localization enhancement," *IEEE Sensors J.*, vol. 18, no. 24, pp. 10208–10216, Dec. 2018.
[36] H. Gan, M. H. B. M. Khir, G. W. Bin Djaswadi, and N. Ramli, "A hybrid model based on constraint OSELM, adaptive weighted SRC and KNN for large-scale indoor localization," *IEEE Access*, vol. 7, pp. 6971–6989, 2019.
[37] L. Jiao, X. Geng, and Q. Pan, "BP k NN: k-nearest neighbor classifier with pairwise distance metrics and belief function theory," *IEEE Access*, vol. 7, pp. 48935–48947, 2019.
[38] M.-L. Zhang and Z.-H. Zhou, "A review on multi-label learning algorithms," *IEEE Trans. Knowl. Data Eng.*, vol. 26, no. 8, pp. 1819–1837, Aug. 2014.

SANDIP BHATTACHARYA received the Ph.D. degree in engineering from the Indian Institute of Engineering Science and Technology (IIEST), Shibpur, India, in 2017. He is currently a Postdoctoral Researcher with HiSIM Research Center, Hiroshima University, Japan. His current research interests include nano device, interconnect modeling, and intelligent circuit design for robotics.

AIWEN LUO (M'18) received the bachelor's degree in engineering from Beijing Jiaotong University, China, in 2009, the master's degree in engineering from Jinan University, China, in 2012, and the Ph.D. degree in engineering from Hiroshima University, Japan, in March 2018, where she has been a Postdoctoral Researcher, since April 2018. Her current research interests include computer vision, pattern recognition, and intelligent robotics.

TAPAS KUMAR MAITI (M'16) received the Ph.D. degree in engineering from Jadavpur University, Kolkata, India, in 2009. He held a postdoctoral position with McMaster University, Hamilton, ON, Canada, for two years, and he spent three years, as a Researcher, and two years, as an Assistant Professor with HiSIM Research Center, Hiroshima University, Japan, where he has been an Associate Professor, since 2017.

SUNANDAN DUTTA received the M.Tech. degree from the Indian Institute of Engineering Science and Technology (IIEST), Shibpur, India, in 2017. He is currently pursuing the Ph.D. degree with the Graduate School of Engineering, Hiroshima University, Japan. His current research interests include humanoid robotics and system cybernetics.

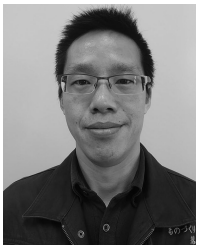

YOSHIHIRO OCHI received the B.Eng. degree from Tottori University, Tottori, Japan, in 2003. Since 2009, he has been with the Technical Center, Hiroshima University, Higashi, Hiroshima, Japan, where he is involved in technical support of the information systems.

MITIKO MIURA-MATTAUSCH (M'96–SM'00–F'07) received the D.Sc. degree from Hiroshima University, Japan. Since 1996, she has been a Professor with Hiroshima University, where she is leading the Ultra-Scaled Device Laboratory.

HANS JÜRGEN MATTAUSCH (M'96–SM'00) received the Ph.D. degree from Stuttgart University, Stuttgart, Germany. Since 1996, he has been a Professor with Hiroshima University, Japan, where he is involved in researching on very large scale integration design, nanoelectronics, and compact modeling.